 CMC, vol.31, no.2, pp.87-111, 2012

Waste Tire Rubberized Concrete Plates for Airport Pavements: Stress and Strain Profiles in Time and Space Domains

E. Ferretti[1]

Abstract: The present study follows a previous study on the stress and strain profiles along the cross-section of waste tire rubberized concrete plates for airport pavements, subjected to quasi-static loads [Ferretti and Bignozzi (2012)]. Further results on the in-situ performance of concrete plain and rubberized taxiways have been collected and presented here. The experimental program has been undertaken at the Guglielmo Marconi airport of Bologna (Italy). It concerns two portions of the taxiway, one built with plain concrete and one with rubberized concrete. Each portion has been fitted with strain gauges embedded in concrete for the acquisition of vertical strains.

Keywords: Waste tire rubberized concrete, Elastic half-space, Environmental pollution.

1 Introduction

The rubberization of concrete by means of waste tires is a viable technique in view of the environmental problem related to the recycling of waste tires. The technique is as much attractive as waste tires are a major concern among waste materials: vulcanization processes make tread rubber particularly resistant to the action of microorganisms, which would employ more than 100 years to degrade a tire completely. Thus, the disposal of tires in landfills is impracticable.

A number of techniques have been proposed in the past for recycling waste tires, which allow for their reuse in non-structural elements, both plastic and cementitious elements. In Ferretti and Bignozzi (2012), recycled waste tires have been used in the mix-design of concrete structural elements for the first time. In particular, the rubberized concrete mixture has been used for preparing a concrete slab to be used in airport pavements. The rubberized concrete was obtained by replacing a 22

[1] DICAM, Facoltà di Ingegneria, Alma Mater Studiorum, Università di Bologna, Viale Risorgimento 2, 40136 (BO), Italy.

Vol.-% of the fine aggregate with rubber scraps, obtained by grinding the tire tread (Fig. 1) and eliminating the metallic fibers of the tread.

The idea of using a rubberized cement concrete mixture for airport pavements comes from the comparison of previous results in terms of strength, fatigue resistance, creep, workability and dynamic characteristics of rubberized and plain concrete, by the author and other researchers [Topçu (1995); Fattuhi and Clark (1996); Fedroff, Ahmad, and Savas (1996); Khatib and Bayomy (1999); Wang, Wu, and Li (2000); Hernandez-Olivaresa, Barluenga, Bollatib, and Witoszek (2002); Bignozzi and Sandrolini (2004); Li, Stubblefield, Gregory, Eggers, Abadie, and Huang (2004); Naik and Siddique (2004); Yang, Kim, Lee, Kim, Jeon, and Kang (2004); Bignozzi and Sandrolini (2005); Ferretti (2005); Ghaly and Cahill IV (2005); Bignozzi and Sandrolini (2006); Ferretti and Di Leo (2008); Zheng, Sharon Huo, and Yuan (2008); Topçu and Sarıdemir (2008); Ferretti (2012a)]. The main properties that make rubberized concrete eligible for airfield pavements are the ability of absorbing impact energy, reducing or minimizing vibration, and delaying cracking and crushing during fatigue cycles more efficiently than traditional concrete. Indeed fatigue is one of the main causes of distress in airfield pavements, where the repetition is lower but the intensity of loads is greater than in highway pavements. Moreover, rubberized concrete is an ideal material for all those structural members for which desired deformability or toughness is more important than strength, such as jersey barriers, road foundations, bridge barriers and, once again, airfield pavements.

Figure 1: Grinding of the tire tread

The small thickness of the slabs and the type of layers chosen for the experimental pavement of the Guglielmo Marconi airport of Bologna (Italy, Fig. 2) [Ferretti and Bignozzi (2012)] allowed us to obtain an intermediate solution between a flexible

Figure 2: Rehabilitation interview of the taxiway at the Guglielmo Marconi airport of Bologna (Italy): area of the rehabilitation interview boxed in red and experimental segment filled in red

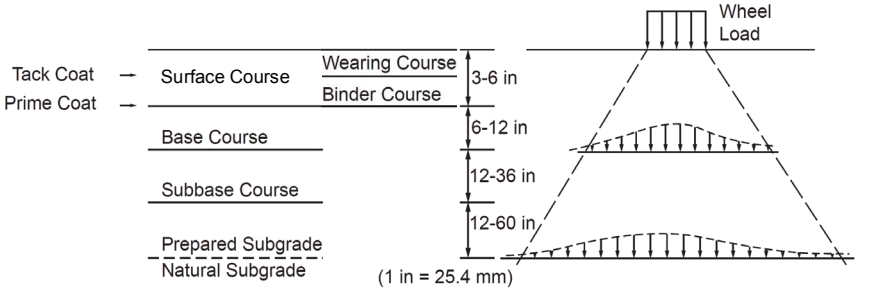

Figure 3: Typical cross session and stress transmission in flexible pavement

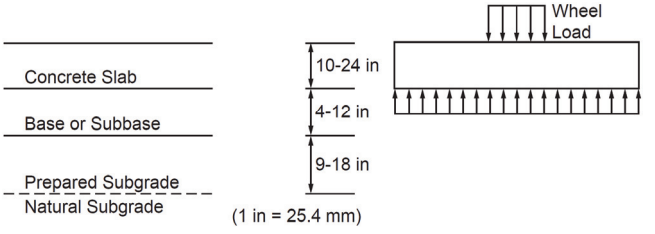

Figure 4: Typical cross section and stress transmission in rigid pavement

(Fig. 3) and a rigid pavement (Fig. 4). We cannot expect concrete pavement to behave like a rigid beam. It is rather a semi-rigid pavement, with some degree of deflection allowed and a mechanism of stress transfer that is intermediate between those showed in Figs. 3 and 4. This is especially true when rubber is added to concrete, since rubberization dramatically decreases the strength of concrete.

The results presented in Ferretti and Bignozzi (2012) concern the strain and stress profiles along two instrumented cross-sections when the gear wheels stand over them. They show that rubberized concrete is more effective than plain concrete in spreading the applied load and distributing it over a large area of the concrete slab/subbase course interface. Here, further results are presented, concerning the stress and strain behavior when the gear wheels move along the two instrumented cross-sections. The stress and strain profiles along the motion direction are also discussed.

2 Experimental set-up

The experimentation has been carried out on the same 14 m length experimental segment of the taxiway of the Guglielmo Marconi airport (Bologna, Italy) showed in Ferretti and Bignozzi (2012) (Fig. 5), which is a flexible taxiway.

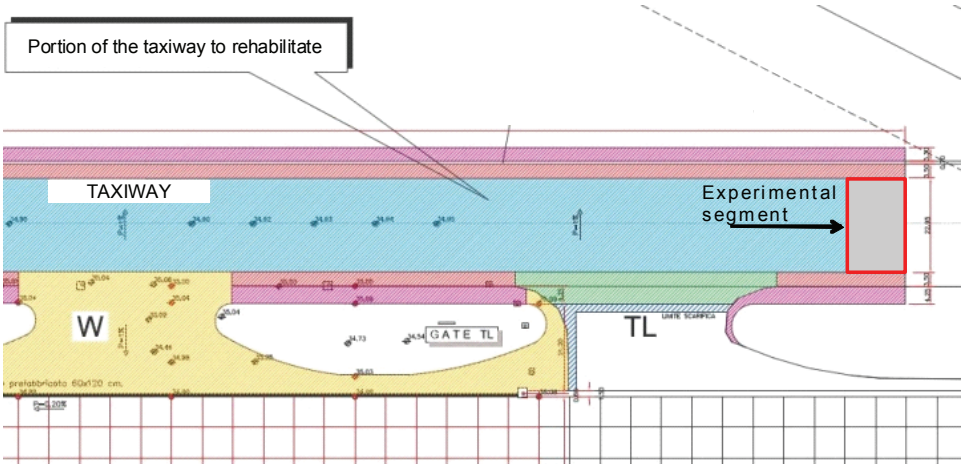

Figure 5: Detail of the rehabilitation interview, with the 14×23 m experimental segment boxed in red

The experimental segment was divided into two sections of 7 m each (Fig. 6), to be realized by substituting the base and binder courses of the flexible pavement (Fig. 3) with a slab of concrete. The reason for this choice lies in the fact that, as

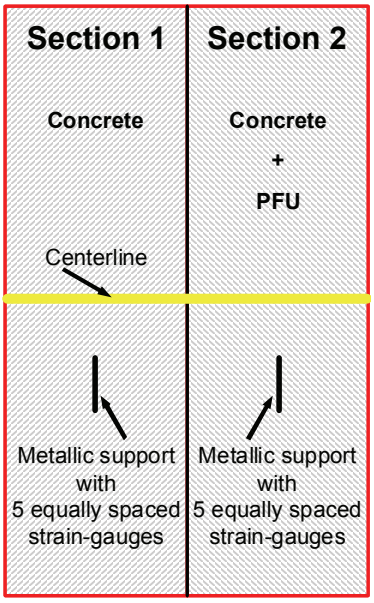

Figure 6: Detail of the experimental segment (boxed area in Fig. 5)

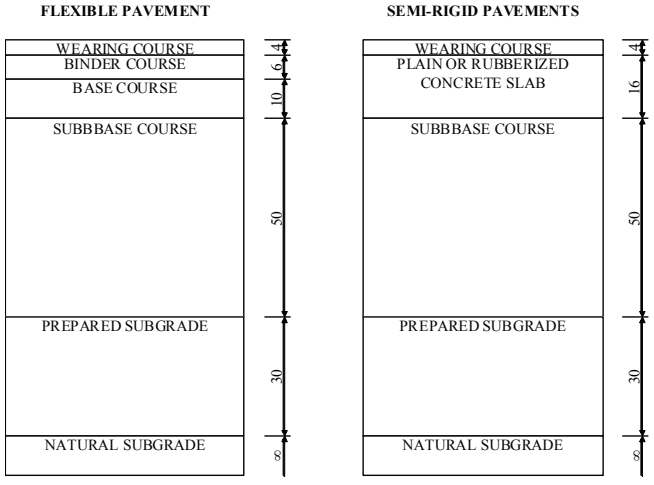

Figure 7: Cross-sections of the taxiway flexible and semi-rigid pavements (dimensions in cm)

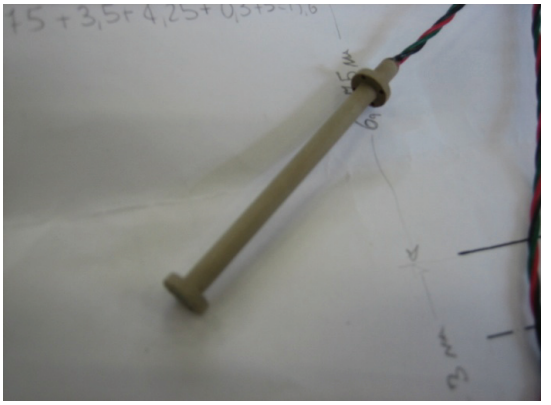

Figure 8: Luchsinger strain-gauge for embedment in concrete

widely discussed in Ferretti and Bignozzi (2012), the taxiway, being considered a critical area, should not be realized with flexible pavement.

The taxiway concrete semi-rigid (rehabilitated) and bituminous flexible (non-rehabilitated) pavements share the same subbase, subgrade and wearing courses (Fig. 7). In the concrete pavement, the base and binder courses were replaced by a slab of plain concrete, in the first section, and rubberized concrete, in the second section (Figs. 6, 7). The plain concrete section of the experimentation has been carried out for comparison purposes, so that we could evaluate how the pavement performance is affected by rubberization. In the following, the control and the rubberized mixture will be named Mixture 1 and Mixture 2, respectively.

The thicknesses of the several layers of the three pavements (the two of the experimentation and the non-rehabilitated one) are shown in Fig. 7. Note how the thickness of the concrete slab ($16\ cm$) is about one third the slab thickness of a rigid pavement for taxiways ($40 \div 50\ cm$), both for Section 1 and 2.

The two sections were instrumented with strain gauges embedded in concrete (Fig. 8). The strain gauges were positioned along two cross-sections, one for each section of the semi-rigid pavement (Fig. 6), so as to acquire the vertical strains due to aircrafts traffic. Only one half of each cross-section was instrumented (Fig. 6). All the strain gauges were connected to a real-time controller, which also allows for remote data acquisition.

The taxiway is an area of highly channelized traffic, due to its low wander width (see Ferretti and Bignozzi (2012) for details). This configures the taxiway as an optimum area for the experimental analysis of the distresses due to repeated loads. Moreover, the high channelization allowed us to identify with a good degree of

Table 1: Percentage annual traffic and track widths for the aircrafts most frequently landing at Bologna

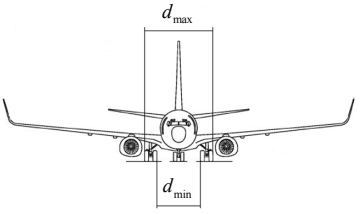

Aircraft	Annual traffic [%]	d_{max} (Max track width) [cm]	d_{min} (Min track width) [cm]
BOEING 737	28.9	641	399
AIRBUS 320	18.3	902	678
CRJ	10	400	176
ATR 42	8.5	467	243
MD 80	8.3	621	397

precision the transverse gear wheel lanes for the aircrafts landing at the Guglielmo Marconi airport.

The aircrafts most frequently landing at the Guglielmo Marconi airport are collected in Tab. 1. Since the distance between right and left wheels of the several aircrafts varies with a constant step (Tab. 1), with five equally spaced strain-gauges arranged along the pavement cross-section as shown in Fig. 9, it is possible to instrument the lanes described by the first, second, fourth and fifth aircrafts of Tab. 1, covering 74% of the annual airport traffic. In particular, with the strain-gauges positioning shown in Fig. 9, at least one strain-gauge is placed just under one lateral wheel or between the two lateral twin wheels each time one of the four analyzed aircrafts passes over the instrumented sections (Fig. 9). Fig 10 shows five of the ten used strain gauges (five for each sections), settled out to be embedded under the five equally spaced lanes. Fig. 10 also shows the metallic support of the strain gauges, which has been walled into the subbase course, fixing its elevation by means of a total station for GPS topographic surveying (Figs. 11, 12).

The metallic support had the function of ensuring the strain gauges were positioned just below the lanes of most channelized traffic (horizontal alignment of the strain-gauges) and just below the upper surface of the concrete slabs (vertical alignment of the strain-gauges) once concreting has been completed. Moreover, the metallic support allowed the strain-gauges to maintain the correct position during concreting (Fig. 13), avoiding strain-gauges overturning and slipping.

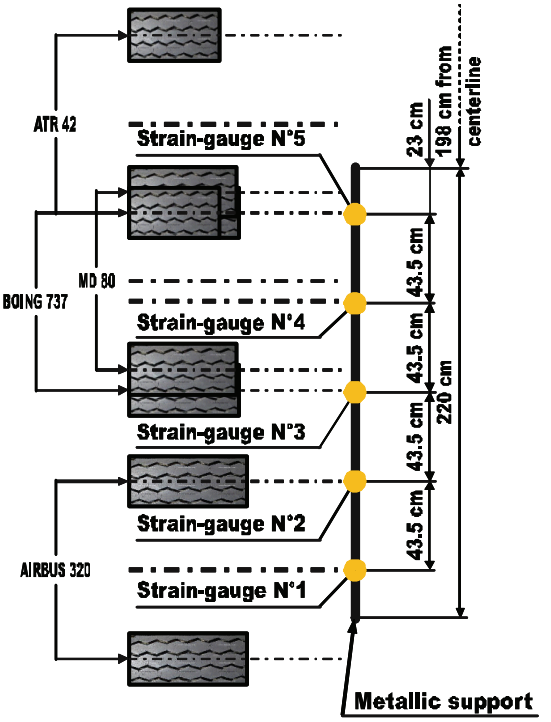

Figure 9: Detail of the metallic support and relative positions of the strain gauges to the wheels of the aircrafts covering 74% of the annual traffic

Figure 10: Positioning of the strain gauges over the metallic support

Figure 11: Base station receiver for GPS topographic surveying positioned on the centerline at the end of the experimental segment

Figure 12: Base of the mobile unit for GPS topographic surveying rested over the metallic support during installation of the metallic support itself

Figure 13: Concreting of Section 2 semi-rigid pavement

Figure 14: Concrete flowing during concreting

Figure 15: Assessment of the fresh concrete workability by means of the Abrams slump test

In order to ensure good concrete flow through the strain-gauges, bars of the metallic support, and cables during concreting (Fig. 14), for both mixtures the desired consistency of fresh concrete was the S5 consistency class, the super fluid class (UNI EN 206-1:2006, UNI 11104:2004), with a laboratory-verified target slump (Fig. 15), of 220 ± 30 *mm* (according to UNI EN 206-1:2006, the tolerance applied to a target slump is ≥ 100 *mm* is ± 30 *mm*). To reach a super fluid consistency, a considerable amount of water is required. This leads to a decrease in strength and resistance to frost and aggressive environments in hardened concrete and to an increased danger of segregation and bleeding. In order to reach a super fluid

Figure 16: Metallic support after concreting

Figure 17: Preparation of cubic and cylindrical specimens while concreting Section 1 semi-rigid pavement

consistency without exceed in quantity of water, we have used a polyacrylic superplasticizer admixture (Axim Creactive LX fluxing agent, see Ferretti and Bignozzi (2012) for details).

Fig. 16 shows the upper part of the metallic support emerging from concrete after concreting. This part has been removed after concrete hardening and before completing the pavement with the wearing course.

3 Experimental results

3.1 Compressive and tensile strength

The specimens used for uniaxial compression tests were cylinders of 15 *cm* (diameter) $\times$ 30 *cm* (high) and cubes of 15 *cm* side. They have been prepared in-situ, during concreting (Fig. 17), and cured in laboratory under controlled thermo-hygrometric conditions.

The ratio between cylindrical and cubic strengths was 0.85 for Mixture 1 and 0.80 for Mixture 2.

Fig. 18 shows the stress-strain relationships for two cubic specimens prepared with Mixture 1 and 2, respectively. The 28 days mean compressive strengths and elastic modules for Mixture 1 and 2 (averaged over 3 cubic specimens) are collected in Tab. 2. The decrement in compressive strength when the rubber is added is well evident from both Fig. 18 and Tab. 2. Nevertheless, as discussed in Ferretti and Bignozzi (2012), it is not essential for airfield applications, since the loads carried by airfield pavements do not overcome the 5% of the collapse load and led the concrete to work in linear-elastic field in both experimental sections.

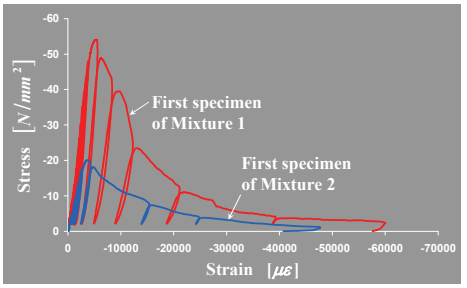

Figure 18: Stress-strain relationships in uniaxial compression for the two mixtures after 28 day curing

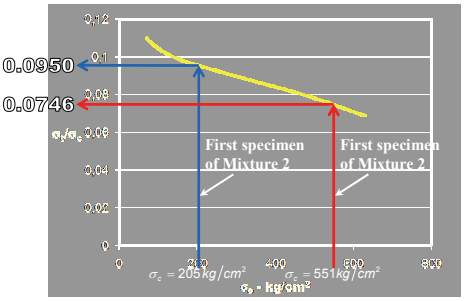

Figure 19: The empirical relationship of Price between the ratio σ_t/σ_c and σ_c

The tensile strength has been evaluated by means of Price's empirical method, which provides the ratio between tensile and compressive strength, σ_t and σ_c respectively, as a decreasing function of σ_c (Fig. 19).

Table 2: Mean mechanical properties of Mixture 1 and 2 after 28 day curing (UNI 9416, UNI EN 12390-1:2002, UNI EN 12390-2:2002, UNI EN 12390-3:2003, UNI 6556:1976)

Mixture 1		Mixture 2	
Compressive strength $\left[N/mm^2\right]$	Elastic modulus $\left[N/mm^2\right]$	Compressive strength $\left[N/mm^2\right]$	Elastic modulus $\left[N/mm^2\right]$
56.07	13573	20.95	7340

From Price's empirical relationship, it follows:

$$\sigma_t = 0.0746\sigma_c = 4.03\ N/mm^2, \tag{1}$$

for the first specimen of Mixture 1 (Fig. 19), where $\sigma_c = 54.06\,N/mm^2 = 551\,kg/cm^2$, and

$$\sigma_t = 0.0950\sigma_c = 1.91\ N/mm^2, \tag{2}$$

for the first specimen of Mixture 2 (Fig. 19), where $\sigma_c = 20.10\,N/mm^2 = 205\,kg/cm^2$.

The complete stress-strain relationships in uniaxial tension for Mixture 1 and 2 (Fig. 20) have been identified for homothety from the stress-strain relationships in uniaxial compression (Fig. 18), with the peak values for the first specimens of Mixture 1 and 2 provided by Eqs. (1) and (2), respectively.

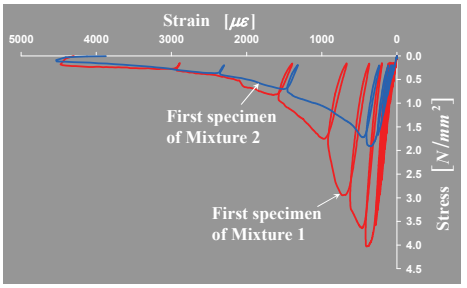

Figure 20: Stress-strain relationships in uniaxial tension for the two mixtures after 28 day curing

Figure 21: Truck used as mobile load

3.2 In-situ acquired data along the motion direction

In the aim of collecting the experimental data in a short period of time, in order to ensure that the data were comparable as far as the climatic conditions are concerned, the data acquisition along the motion direction has been carried out by night, when the aircraft traffic is quite irrelevant, using our truck for geotechnical survey (Fig. 21) as mobile load. The second advantage connected to the use of a truck instead of waiting for an aircraft passage is the possibility of pre-fixing and keeping the velocity of the mobile load constant throughout the test. The selected truck speed was 2.7 km/h.

The front wheels of the truck are single wheels, while the back wheels are twin wheels (Fig. 21), like the gear wheels in aircrafts. Each single and twin wheel transmits a load of 34 kN and 27 kN, respectively, to the pavement.

The truck has passed twice (in going and return) over each strain-gauge, coming back in reverse. In the first passage (Fig. 22), the right wheels of the truck have passed twice over the strain-gauges N° 5, the ones nearest to the centerline (Fig. 9), of both Section 1 and 2. In the second passage the right wheels have passed twice over the strain-gauges N° 4 and so on, until the fifth passage, when the right wheels have passed twice over the strain-gauges N° 1 and the left wheels have passed twice very near to the strain-gauges N° 5, since the distance between the right and left wheels is comparable to the distance between the strain-gauges N° 1 and 5.

The strains acquired by the strain-gauges N° 5 of Section 1 and 2 during the five passages are shown in Fig. 23, where G stands for going and R stands for return. In the first-order approximated uniaxial assumption:

$$\sigma = E\varepsilon, \tag{3}$$

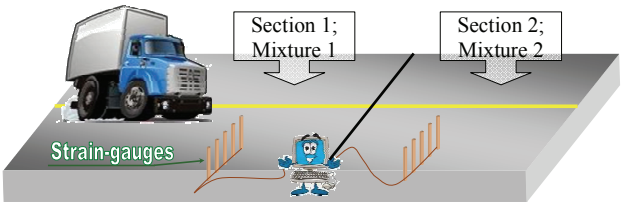

Figure 22: Truck path during the first passage, loading the strain-gauges N° 5 of both Sections 1 and 2

with E being Young's modulus, or elastic modulus (Tab. 2), where the strains in Fig. 23 are negative a further state of compression adds to the preexisting compressive stress field, due to the weigh of the wearing course, while, where the strains are positive, a state of tension superimposes. Depending on the thickness of the wearing course, the resulting stress filed after superimposition may be of compression (high thickness) or tension (low thickness). In order to simulate the most severe condition for the pavement, the weight of the wearing course will be neglected in the following.

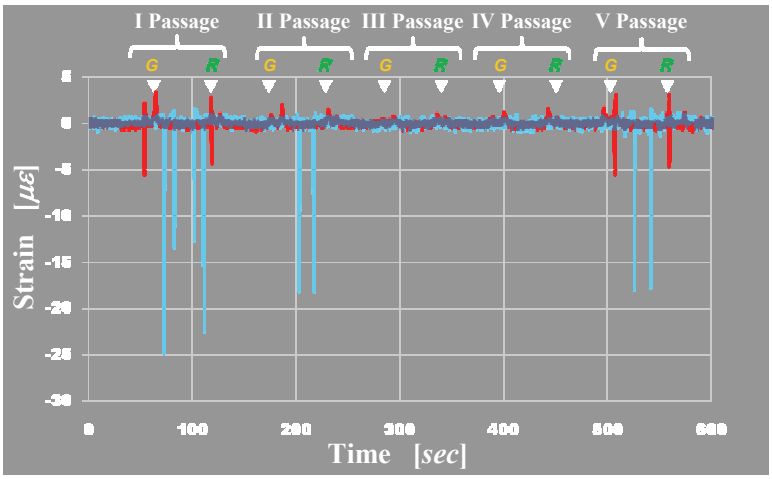

Figure 23: Data acquired by the strain-gauges N° 5 of Section 1 (plain concrete), in red, and 2 (rubberized concrete), in blue

If compared with Figs. 18 and 20, Fig. 23 shows that the strains induced by the mobile load are small enough for leading Sections 1 and 2 to work in linear-elastic field, both in compression and in tension. Moreover, the negative peaks in Section

2 (blue) are greater than the negative peaks in Section 1 (red) induced by the same load, since the elastic modulus in uniaxial compression of Mixture 2 is lower than the elastic modulus in uniaxial compression of Mixture 1 (Fig. 18, Tab. 2).

The greater strain values in Fig. 23 have been acquired by the strain-gauges N° 5 during the first passage, when the right wheels of the truck pass just over the acquiring strain-gauge. The acquired strains are well appreciable even during the second passage, when the right wheels pass over the strain-gauge N° 4, the nearest to that of acquisition. Finally, the peaks observed during the fifth passage are due to the left wheels, which are approaching the acquiring strain-gauge.

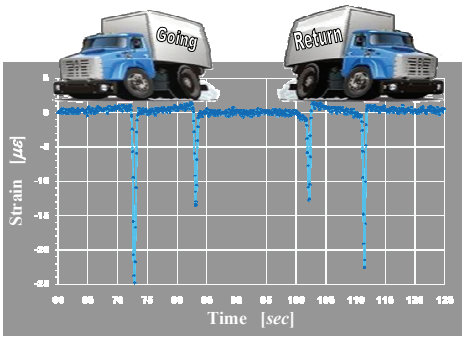

Figure 24: Detail of the first passage over the strain-gauge N° 5 of the second section

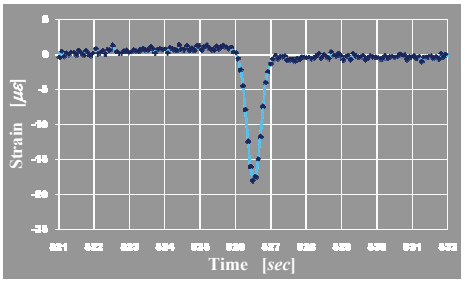

Figure 25: Vertical strain behavior in function of the time when a wheel passes in going over a strain-gauge of the second section

For each passage in Fig. 23, the first negative peaks in going (first red peak and first blue peak) are due to the passage of the front wheels, while the second negative peaks in going are due to the passage of the back wheels (Fig. 24). Moreover, since the return has been made in reverse, the first negative peaks in return are due to the passage of the back wheels, while the second negative peaks in return are due to the passage of the front wheels (Fig. 24). The negative peaks due to the passage of the front wheels are greater than the negative peaks due to the passage of the back wheels, in that the load transmitted by the front wheel is greater than the load transmitted by the back wheels.

Each time a wheel has passed in going over a strain-gauge, both of Section 1 or 2, a recurrent behavior has been observed (see Fig. 25 for Section 2): at first, when the wheel was approaching the strain-gauge, a weak positive strain has appeared in the pavement, then, at the passage of the wheel over the strain-gauge, the strain became negative and reached its maximum absolute value, and finally, when the wheel was

leaving the strain-gauge, the strain gradually returned to assume its undisturbed condition value.

The acquired positive strains do not seem to be caused by friction forces developed at the interface between the pavement and the wheel, since they appear even when the truck speed is very low, that is, in quasi-static conditions. In this last case, the vertical strain profile of Fig. 25 becomes symmetric with respect to the wheel and exhibits two positive peaks of equal intensity, one before and one after the wheel. Consequently, we may conclude that friction is not the main cause of the growing of a positive state of strain inside the pavement, but interacts with it enhancing the positive strains from one side of the wheel and decreasing the positive strains from the other side. In other words, the vertical load has a symmetric effect on the positive strains, while friction has an anti-symmetric effect on them. The behavior of the vertical strain profile along the motion direction comes from the superimposition of these two effects, with the second effect depending on the truck speed.

The increase of tensile stresses when a load moves along a concrete pavement has been assumed by several researchers, in the past [Spangler (1935); Hossain, Muqtadir and Hoque (1997); Darestani, Thambiratnam, Baweja and Nataatmadja (2006)], in order to explain some of the main mechanisms of pavement distress, but never actually experimentally identified inside pavements, to the knowledge of the author. Moreover, since now the tensile stresses induced into pavements by moving loads have always been assumed as longitudinal or transverse stresses (horizontal stresses in both cases). Here, the identified tensile stresses are vertical stresses. Thus, for the first time this work provides an experimental evidence that a tensile state of vertical stress exists in vehicular loaded pavements and provides information on how rubberization acts on it. Actually, in Fig. 23 we can appreciate that, while the negative peaks are greater in rubberized than in plain concrete, due to the greater deformability of rubberized concrete, the opposite happens for positive peaks, which are smaller for rubberized than for plain concrete.

By observing Fig. 23 we can also evaluate the effect of single rather than twin wheels on the tensile state of stress arising into the pavement, since the tensile peaks for the passage of a front single wheel (first peaks in going and second peaks in return) are smaller than the tensile peaks for the passage of a back twin wheel (second peaks in going and first peaks in return), both for Mixture 1 and 2 (for Mixture 2, see the detail in Fig. 24 for major clarity). Thus, the twin wheels interact in a way to enhance the tensile state of stress in concrete pavements, while the compressive state of stress is decreased.

From the knowledge of the truck speed, which has been pre-fixed, it was possible to pass from the time/strain diagrams to the space/strain diagrams. The space/strain diagram associated to Fig. 25 has been plotted in Fig. 26, where the horizontal axis

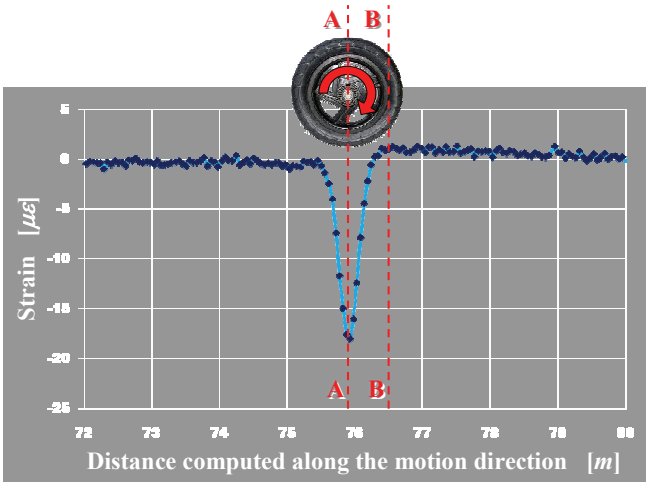

Figure 26: Vertical strain behavior in function of the distance when a wheel passes in going over a strain-gauge of the second section

coincides with the motion direction and is positively oriented as the gear direction. In Fig. 26, the positive peak is well evident in front of the wheel [Ferretti (2012b)].

By comparing the data acquired in the same instant from the five strain-gauges of the same instrumented cross-section, it is possible to build the behavior of strains along each cross-section. The most interesting cross-sections are the ones passing from the compressive and tensile peaks, the **A**-**A** and **B**-**B** sections in Fig. 26 respectively. The behavior of strains along the **A**-**A** cross-section has been already discussed for a front single wheel in Ferretti and Bignozzi (2012). Here, the strain profile for a front single wheel (Fig. 27) is compared to the strain profile for a back twin wheel (Fig. 28).

As previously pointed out, the maximum strain for twin wheels is lower than the maximum strain for single wheel, due to the lower load transmitted by twin wheels to the pavement. Besides this, the strain profile around the peak is flatter for twin than for single wheels, due to the superimposition of strains induced by both twin wheels. Thus, from the comparison between Figs. 27 and 28 we can conclude that the use of twin instead of single wheels is advantageous as far as the negative state of strain is concerned, since strains are lower and distributed more uniformly on the pavement. Finally, as for single wheels [Ferretti and Bignozzi (2012)], also for twin wheels strains are spread over a greater area for Mixture 2 than for Mixture 1 (Fig. 28). This means that strain curves of different airfields overlap on a greater portion for Mixture 2 as compared with Mixture 1, limiting the arising of traffic

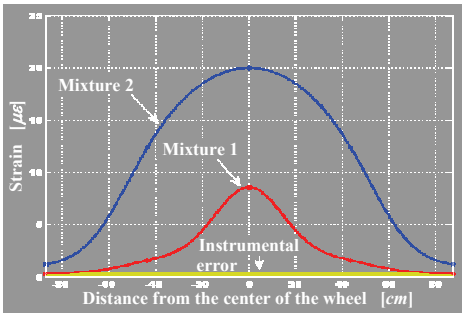

Figure 27: Profiles of vertical strains, in absolute value, induced by the passage of a front single wheel along the **A**-**A** cross-section

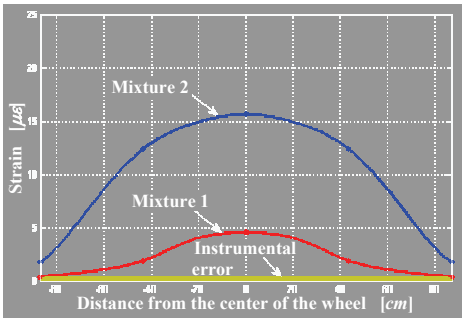

Figure 28: Profiles of vertical strains, in absolute value, induced by the passage of a back twin wheel along the **A**-**A** cross-section

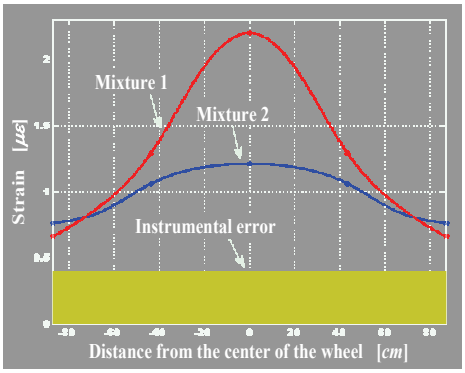

Figure 29: Vertical strain profiles along the **B**-**B** cross-section induced by the passage of a front single wheel

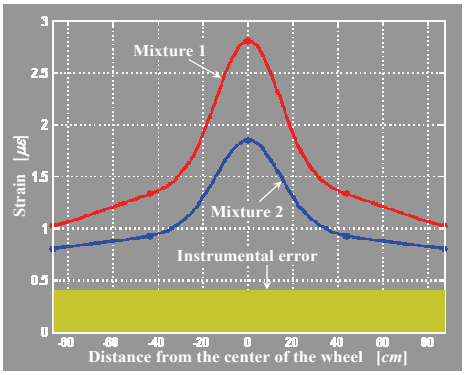

Figure 30: Vertical strain profiles along the **B**-**B** cross-section induced by the passage of a back twin wheel

lanes, thus improving the rutting performance of concrete pavements.

As far as the behavior of strains along the **B**-**B** cross-section is concerned, the comparison between the strain profiles plotted for single wheels, in Fig. 29, and twin wheels, in Fig. 30, shows that rubberization is effective in limiting the growth of a tensile state of stress particularly under twin wheels. Actually, the tensile stresses in Section 2, besides being smaller than in Section 1, go to zero more quickly than in Section 1 when they are computed under twin rather than single wheels. Consequently, for twin wheels positive strains are spread over a smaller area for Mixture 2 than for Mixture 1.

Since the involved positive strains are not great enough to make the problem of the permanent strains relevant, the dimension of the positively strained area has not any effect on the rutting performance of concrete pavements. Having a smaller positively strained area means having a lower percentage of pavement surface subjected to strains of opposite sign, alternatively, during the passage of a wheel. Consequently, the use of rubberized instead of plain concrete under twin wheels is advantageous as far as the positive state of strain is concerned, since strains are lower and distributed on a smaller area of the pavement. Since the gear wheels are just twin wheels, this last point gives useful design information to be spent for airfield pavements.

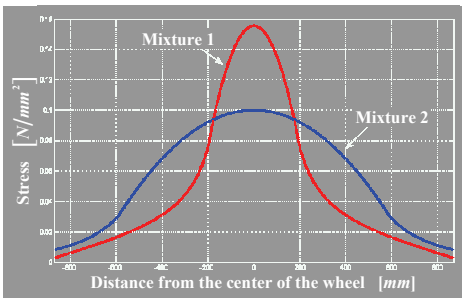

Figure 31: Profiles of vertical stresses, in absolute value, induced by the passage of a front single wheel along the **A**-**A** cross-section

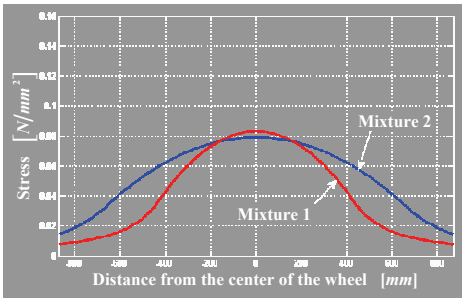

Figure 32: Profiles of vertical stresses, in absolute value, induced by the passage of a back twin wheel along the **A**-**A** cross-section

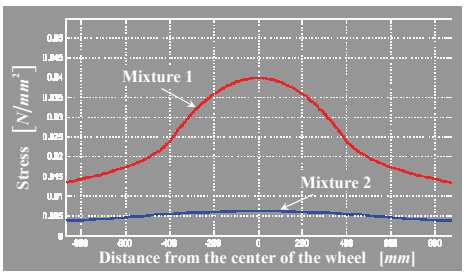

Figure 33: Vertical stress profiles along the **B**-**B** cross-section induced by the passage of a front single wheel

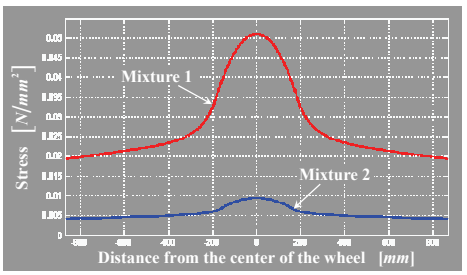

Figure 34: Vertical stress profiles along the **B**-**B** cross-section induced by the passage of a back twin wheel

As done in Ferretti and Bignozzi (2012), the stress profiles have been obtained from the strain profiles in the first-order approximated uniaxial assumption (Eq. 3).

As for the stress profiles induced by single wheels along the **A**-**A** cross-section, discussed in Ferretti and Bignozzi (2012) and recalled in Fig. 31 for comparison, also in the stress profiles induced by twin wheels along the **A**-**A** cross-section the peak stress is lower in Mixture 2 than in Mixture 1 (Fig. 32), despite strains are higher for Mixture 2 than for Mixture 1 (Fig. 28). Once more, this happens since k_E, the ratio between E_2, the elastic modulus of Mixture 2, and E_1, the elastic modulus of Mixture 1:

$$k_E = \frac{E_2}{E_1}, \tag{4}$$

is lower than k_ε, the ratio between the peak strains of Mixture 1 and 2, ε_1 and ε_2 respectively:

$$k_\varepsilon = \frac{\varepsilon_1}{\varepsilon_2}. \tag{5}$$

Consequently:

$$\sigma_2 = E_2\varepsilon_2 = k_E E_1 \varepsilon_2 = \frac{k_E}{k_\varepsilon} E_1 \varepsilon_1 = \frac{k_E}{k_\varepsilon}\sigma_1 < \sigma_1, \tag{6}$$

where σ_1 is the peak stress in Mixture 1, σ_2 is the peak stress in Mixture 2, and

$$k_E < k_\varepsilon \Rightarrow \frac{k_E}{k_\varepsilon} < 1. \tag{7}$$

Moreover, the stress curve for Mixture 2 is smoother than that of Mixture 1 even for twin wheels. This follows in lower stress gradients for Mixture 2 than for Mixture 1. Since a high stress gradient is one of the main causes of distress for repeated loads, it is reasonable to expect a longer economic life for Mixture 2 than for Mixture 1.

The stress profiles along the **B**-**B** cross-section are shown in Figs. (33), for single wheels, and (34), for twin wheels. Obviously, the advantage connected to the use of rubberized concrete is more evident along the **B**-**B** cross-section than along the **A**-**A** cross-section, since strains are already lower for Mixture 2 than for Mixture 1 (Figs. 29 and 30) and, when the stresses are identified from the strains, the ratio between the elastic modules contributes to increase the gap between the curves of plain and rubberized concrete, flatting the curves of rubberized concrete considerably.

From the comparison between Fig. (33), where the involved stresses are positive, and Fig. (31), where the involved stresses are negative, we can conclude that the use of rubberized instead of plain concrete is advantageous for single wheels, since it leads to a reduction (in absolute value) of stresses, both of tensile and compressive

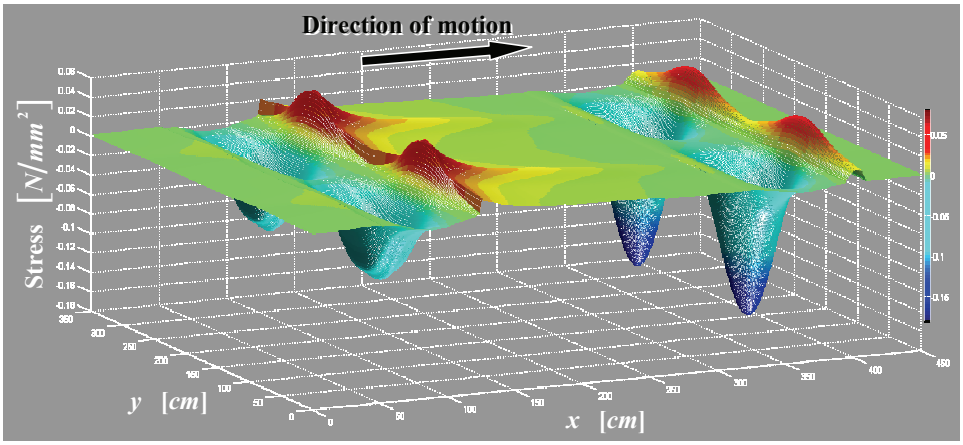

Figure 35: Vertical stresses under the wheel-print for plain concrete

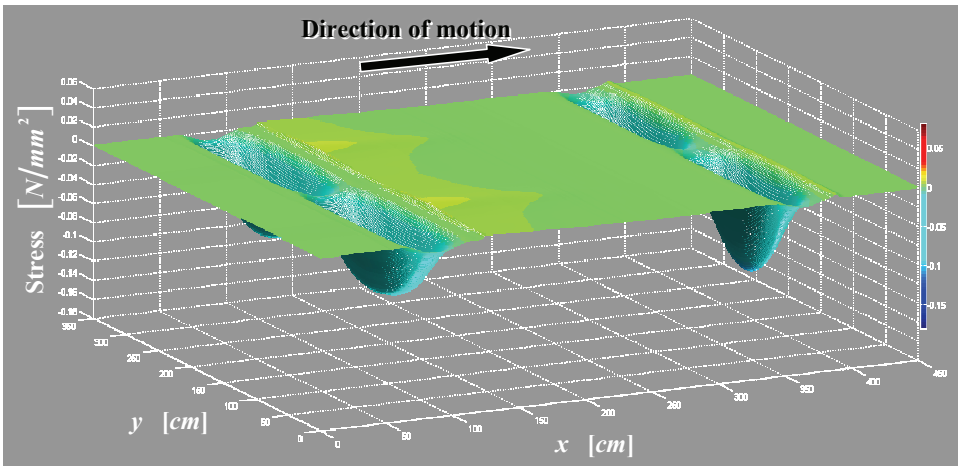

Figure 36: Vertical stresses under the wheel-print for rubberized concrete

nature, and the advantage is much more sensitive for tensile than for compressive stress profiles. The same can be concluded for twin wheels, from the comparison between Figs. (34) and (32). It is worth noting that having a decreased state of tensile stress is particularly remarkable, since just tensile stresses induced by moving loads are one of the main causes of premature distress of concrete pavements.

By interpolating the stress profiles both along the motion direction and the cross-sections, it was possible, finally, to obtain the stress behavior under the wheel-print for plain (Fig. 35) and rubberized concrete (Fig. 36).

4 Conclusions

A rubberized cement concrete mixture has been used for preparing a concrete slab customarily used for rigid pavements, but the subbase and subgrade courses were those typical of a flexible pavement and the concrete slab thickness was much smaller than that of a rigid pavement. A second slab has been prepared with a control plain concrete mixture, for comparison purposes. Both slabs have been fitted with strain-gauges embedded in concrete very near to the slab surface, in order to investigate the complex state of vertical strain of the superficial pavement layers and identify the related vertical stress field. Moreover, having used a truck provided of both single and twin wheels as mobile load, it was possible to estimate the effect of the wheel configuration on the induced vertical strains and stresses.

One of the main results of the experimentation concerns the identification of a tensile state of vertical stress induced into the pavement by mobile loads, since the existence of tensile vertical stresses has been never experimentally verified previously. Since tensile stresses must be kept as low as possible in concrete, it is of primary importance to evaluate how the use of a rubberized instead of a plain concrete mixture or single instead of twin wheels acts on them. It has been found that twin wheels act negatively on the tensile state of stress, enhancing it, while rubberization acts positively, reducing it. Twin wheels are used more and more frequently, due to the constant growth of aircraft dimensions, and constitute the major part of gear wheels. This makes the ability of decreasing tensile stresses of rubberized concrete particularly interesting.

When coupled with twin wheels, rubberized concrete is effective also in decreasing the peak compressive vertical stress and increasing the rutting performance of concrete pavements. Thus, we may conclude that rubberization ameliorates the performance of concrete pavements as far as its behavior both in tension and compression.

The choice of a Mixture instead of another cannot be based on the stress field induced into mixtures by load exclusively, of course. The stress field must be related

to the compressive and tensile strength of mixtures, before deciding what mixture to use. Nevertheless, since the involved stresses are very far from the compressive and tensile strength for both Mixtures, the difference between compressive strengths in plain and rubberized concrete, from one hand, and tensile strengths in plain and rubberized concrete, on the other hand, can be neglected. This means that the choice may be done by comparing Figs. 35 and 36 directly, with the criterion of preferring the Mixture giving the lower state of tensile stress when loaded by vehicular traffic. As can be checked in Figs. 35 and 36 easily, the mixture satisfying this criterion is the rubberized one.

5 Future developments

The tensile state of stress identified into the pavement is not justified by Boussinesq's closed elastic solution for a homogeneous, linear-elastic and isotropic half-space subjected to a point-load perpendicular to the surface [Boussinesq (1876); Boussinesq (1885)], directly or indirectly used for airfield pavement design. Neither are more refined models and empirical methods [Fröhlich (1934); Burmister (1943); Westergaard (1943); Odemark, (1949); Söehne (1958); Veverka, (1973); Binger and Wells (1989); Sharifat and Kushwaha (2000); Barker and Gonzalez, (2006); Gonzales (2006); Seyrafian, Gatmiri and Noorzad (2007); Caron, Theillout and Brill (2010)] able to account for tensile stresses.

In Ferretti and Bignozzi (2012), it was already pointed out how Boussinesq's closed elastic solution does not provides information even on the relationship between the elastic parameters of the medium and the stress profiles along the cross-section, relationship which has been experimentally verified just in Ferretti and Bignozzi (2012). Since the existence of tensile stresses is actually compatible with some distress mechanisms of concrete pavements, the present experimentation, together with the findings of Ferretti and Bignozzi (2011, submitted), seem to suggest a revision of Boussinesq's closed elastic solution [Ferretti (2012b)]. This may lead to a better comprehension of the stress field induced by an aircraft to airfield pavements. In particular, it may clarify the mechanism of stress transfer near the surface for static and dynamic loads, that seems not to be sufficiently exploited at present, as extensively discussed in Ferretti and Bignozzi (2012). In perspective, the enhanced theory of Boussinesq may lead to formulate a more realistic criterion of design for airfield pavements, which better accounts for stresses and deflections than the methods currently used.

Acknowledgement: The SAB staff – infrastructures development, Guglielmo Marconi Airport of Bologna (Italy), and, especially, Domenico Terra, Engineer, are gratefully acknowledged for having assigned the taxiway of the airport to the

experimentation of the new proposed airfield pavement. Eng. Adriano Cirasole is also acknowledged for his active contribution in data processing.

References

Barker, W.R., Gonzalez, C.R. (2006): *Independent Evaluation of 6-Wheel Alpha Factor Report*. Letter Report to the Federal Aviation Administration, U.S. Army Engineer Research and Development Center, Vicksburg, Mississippi.

Bignozzi, M.C., Sandrolini, F. (2004): Recycling tyre rubber in building materials. Proc. *International Conference: Sustainable Waste Management and Recycling: Used/Post-Consumer Tyres*, Kingston University, London, September 14–15 2004, Thomas Telford, London, pp. 77–84.

Bignozzi, M.C., Sandrolini, F. (2005): Il riciclo di pneumatici particellati come aggregati fini in malte cementizie auto compattanti. Proc. *Seminari di Ecomondo 2005*, Maggioli Editore, 26-29 Ottobre 2005, Rimini, pp. 41–46.

Bignozzi, M.C., Sandrolini, F. (2006): Tyre rubber waste recycling in self-compacting concrete. *Cement Concrete Res*., vol. 36, pp. 735–739.

Binger, R.L., Wells, L.G. (1989): *Simulation of compaction from surface mining systems*. ASAE Paper no. 89-2018, St. Joseph, MI: ASAE.

Boussinesq, M.J. (1876): *Essai théorique sur l'équilibre d'élasticité des massifs pulvérulents compare à celui de massifs solides et sur la poussée des terres sans cohésion*. Mémoires des Savants Etrangers, Académie de Belgique, 40, Bruxelles.

Boussinesq, M.J. (1885): *Application des potentiels a l'étude de l'équilibre et du mouvement des solides élastiques, avec des notes étendues sur divers points de physique mathématique et d'analyse*. Gauthier-Villars imprimeur libraire, Paris.

Burmister D. M. (1943): The Theory of Stresses and Displacements in Layered Systems and Applications to the Design of Airport Runways. Proc. *Highway Research Board*, vol. 23.

Caron, C., Theillout, J.N., Brill, D.R. (2010): Comparison of US and French Rational Procedures for the Design of Flexible Airfield Pavements. Proc. *2010 FAA Worldwide Airport Technology Transfer Conference*, Atlantic City, New Jersey, USA, April 2010, 23 pp.

Darestani, M.Y., Thambiratnam, D.P., Baweja, D., Nataatmadja, A. (2006): Dynamic Response of Concrete Pavements under Vehicular Loads. *Proceedings IABSE Symposium*, Budapest, Hungary, 2006, 8 pp.

Fattuhi, N.I., Clark, L.A. (1996): Cement-based materials containing shredded scrap truck tyre rubber. *Constr. Build. Mater*., vol. 10, no. 4, pp. 229–236.

Fedroff, D., Ahmad, S., Savas, B.Z. (1996): Mechanical properties of concrete

with ground waste tire rubber. *Transportation Research Board 1996; Report No. 1532*, pp. 66–72.

Ferretti, E. (2005): A Local Strictly Nondecreasing Material Law for Modeling Softening and Size-Effect: a Discrete Approach. *CMES: Computer Modeling in Engineering & Sciences*, vol. 9, no. 1, pp. 19-48.

Ferretti, E. (2012a): Shape-effect in the effective laws of Plain and Rubberized Concrete. *CMC: Computers, Materials & Continua*, vol. 30, no. 3, pp. 237-284.

Ferretti, E. (2012b): A Higher Order Solution of the Elastic Problem for a Homogeneous, Linear-Elastic and Isotropic Half-Space Subjected to a Point-Load Perpendicular to the Surface. *CMES: Computer Modeling in Engineering & Sciences*, vol. 86, no. 5, pp. 435-468.

Ferretti, E., Bignozzi, M.C. (2012): Stress and Strain Profiles along the Cross-Section of Waste Tire Rubberized Concrete Plates for Airport Pavements. *CMC: Computers, Materials & Continua* vol. 27, no. 3, pp. 231-274.

Ferretti, E., Di Leo, A. (2008): Cracking and Creep Role in Displacement at Constant Load: Concrete Solids in Compression. *CMC: Computers, Materials & Continua*, vol. 7, no. 2, pp. 59–80.

Fröhlich, O.K. (1934): *Druckverteilung im Baugrunde*. Springer Verlag, Wien.

Ghaly, A.M., Cahill IV, J.D. (2005): Correlation of strength, rubber content, and water to cement ratio in rubberized concrete. *Can. J. Civil. Eng*., vol. 32, no. 6, pp. 1075–1081.

Gonzales, C.R. (2006): Implementation of a New Flexible Pavement Design Procedure for U.S. Military Airports. Proc. *Fourth LACCEI International Latin American and Caribbean Conference for Engineering and Technology* (LACCEI'2006), Mayagüez, Puerto Rico, 21-23 June 2006, 2006, 10 pp.

Hernandez-Olivaresa, F., Barluenga, G., Bollatib, M., Witoszek, B. (2002): Static and dynamic behaviour of recycled tyre rubber-filled concrete. *Cement Concrete Res*., vol. 32, no. 10, pp. 1587–1596.

Hossain, M., Muqtadir, A., Hoque, A.M. (1997): Three-Dimensional Finite Element Analysis of Concrete Pavement System. *Journal of Civil Engineering*, the Institution of Engineers, Bangladesh, vol. CE 25, No. 1, pp. 33–47.

Khatib, Z.K., Bayomy, F.M. (1999): Rubberized Portland cement concrete. *J. Mater. Civil. Eng*., vol. 11, no. 3, pp. 206–213.

Li, G.Q., Stubblefield, M.A., Gregory, G., Eggers, J., Abadie, C. and Huang, B.S. (2004): Development of waste tire modified concrete. *Cement Concrete Res*., vol. 34, no. 12, pp. 2283–2289.

Naik, T.R., Siddique, R. (2004): Properties of concrete containing scrap tire rub-

ber – an overview. *Waste Manage*, vol. 24, no. 6, pp. 563–569.

Odemark, N. (1949): *Undersökning av elasticitetegenskaperna hos olika jordarter samt teori för beräkning av belägningar enligt elasticitetsteorin*. Statens Väginstitut, meddelande 77.

Seyrafian, S., Gatmiri, B., Noorzad, A. (2007): Analytical Investigation of Depth Non-homogeneity Effect on the Dynamic Stiffness of Shallow Foundations. *CMES: Computer Modeling in Engineering & Sciences*, vol. 21, no. 3, pp. 209–217.

Sharifat, K., Kushwaha, R. L. (2000): *Modeling soil movement by tillage tools*. Saskatoon, Saskatchewan Canada: Department of Agricultural and Bioresource Engineering, University of Saskatchewan.

Söehne, W. (1958): Fundamentals of pressure distribution and soil compaction under tractor tires. *Agricultural Engineering*, vol. 39, pp. 276–281.

Spangler, M.G. (1935): Stresses in Concrete Pavement Slabs. *Transportation Research Board of the National Academies – Highway Research Board Proceedings*, vol. 14, No. Pt1.

Topçu, I.B. (1995): The properties of rubberized concretes. *Cement Concrete Res.*, vol. 25, no. 2, pp. 304–310.

Topçu, I.B., Sarıdemir, M. (2008): Prediction of rubberized concrete properties using artificial neural network and fuzzy logic. *Construction Build. Mater.*, vol. 22, pp. 532–540.

Veverka V. (1973): *Modules, contraintes et déformations des massifs et couches granulaires*. Rapport de Recherche, no. 162, vv, Centre de Recherches Routières, Bruxelles.

Wang, Y., Wu, H.C., Li, V.C. (2000): Concrete reinforcement with recycled fibers. *J. Mater. Civil. Eng.*, vol. 12, no. 4, pp. 314–319.

Westergaard, H.M., (1943): New Formulas for Stresses in Concrete Pavements of Airfields. *ACE Transactions*, vol. 108. Also in *ACE Proceedings*, vol. 73, no. 5, May, 1947.

Yang, H.S., Kim, D.J., Lee, Y.K., Kim, H.J., Jeon, J.Y., Kang, C.W. (2004): Possibility of using waste tire composites reinforced with rice straw as construction materials. *Bioresource Technol.*, vol. 95, pp. 61–65.

Zheng, L., Sharon Huo, X., Yuan, Y. (2008): Experimental investigation on dynamic properties of rubberized concrete. *Constr. Build. Mater.*, vol. 22, pp. 939–947.